Available online at www.sciencedirect.com
SCIENCE DIRECT
Thin Solid Films 506–507 (2006) 460 – 463
thin solid films
www.elsevier.com/locate/tsf

Low impedance antenna arrangement of internal linear ICP source for large area FPD processing

S.J. Jung *, K.N. Kim, G.Y. Yeom

Department of Materials Science and Engineering, Sungkyunkwan University, Suwon 440-746, Korea

Available online 12 September 2005

Abstract

In this study, two different types of internal linear antennas were compared and their characteristics were investigated for a large area ICPs applied to FPD processing. The measured plasma density for the double comb-type antenna was higher than $2 \times 10^{11}/cm^3$ and the etch rates of photoresist and SiO_2 at 5000 W rf power, −60 V of dc-bias voltage, and 15 mTorr SF_6 were about 3000 Å/min and 1500 Å/min. The etch non-uniformity of the photoresist within the substrate was about 7% at 5000 W of rf power.

Keywords: Plasma; Langmuir; Uniformity

1. Introduction

Currently, plasma processing is widely applied, not only to semiconductor device processing but also to FPD manufacturing processes [1–3]. The most common requirements for the plasma sources applied to semiconductor and FPD processing are high and uniform densities of ions and active species, low damage to the substrates, and reproducibility, etc. [4]. ICPs with external antenna coils have be proven to meet the above requirements [5–7]. However, due to the extremely large substrate sizes of FPD processing, the scaling up of the plasma sources for the FPD processing is one of the key challenges for the next generation FPD processing. The conventional ICPs having a multi-turn spiral antenna coil has reached its limit in extending the process area due to its large impedance, which causes a large voltage differences between the ends of the antenna, the thick dielectric window between the plasma and the antenna for the electromagnetic wave transmission, and the standing wave effect. Therefore, conventional ICPs using the external spiral antenna has shown problems in extending the process area [8].

One of the solutions to the above problems is to use internal-type ICPs [9]. Currently, various internal-type ICPs utilizing serpentine-type antennas have been reported for the applications of large area FPD processing [10,11]. However, the serpentine-type antenna could exhibit a standing wave effect which results in unstable and non-uniform plasmas with increasing antenna length. To reduce the standing wave effect, lower impedance internal-type antennas such as the antennas investigated by Y. Setsuhara et al. [12] should be used.

In this study, serpentine-type and double comb-type for a lower antenna impedance were studied for the dry etching application of the next generation of large area FPD.

2. Experiment

Fig. 1 shows schematic diagrams on the arrangements of the two different types of linear internal-type ICPs used in this experiment. For the serpentine-type antenna shown in the top of the figure, five linear antennas were connected in series and the radio frequency (rf) power was connected to one end while the other was connected to the ground. The total length of the antenna was about 7 m. In the case of the double comb-type antenna, each end of the five internal antennas was connected to the rf power and the ground, alternatively, as shown in the bottom of the figure.

The characteristics of the plasma were investigated using a Langmuir probe (Hiden Analytical Inc. ESP) located 7.5

* Corresponding author.
E-mail address: jungsj@skku.edu (S.J. Jung).

0040-6090/$ - see front matter © 2005 Elsevier B.V. All rights reserved.
doi:10.1016/j.tsf.2005.08.047

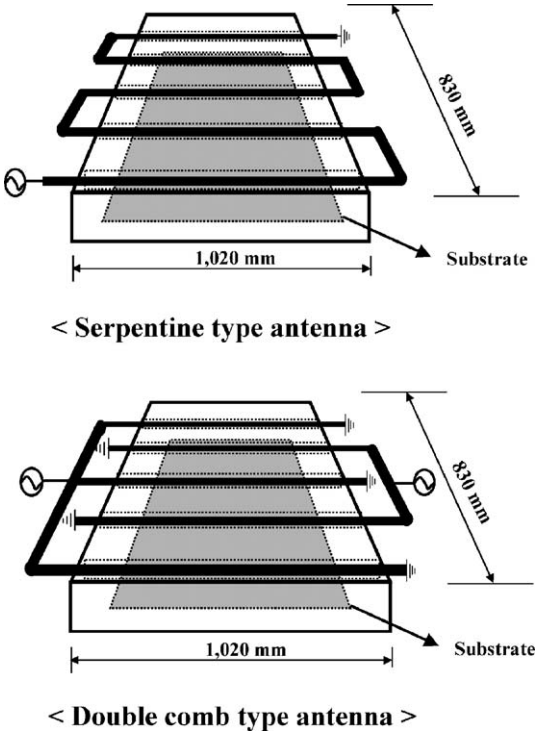

Fig. 1. Schematic diagram of the serpentine and double comb-type antennas used in the experiment.

cm below the plasma sources. Rf voltage and the dc voltage at the surface of the quartz tubing were measured using a high voltage probe (Tektronix P6015A). The rf voltage at the matching network was also measured using a V–I probe (ENI 1065 M2).

3. Results and discussion

Fig. 2 shows the antenna rf rms voltages measured by the high voltage probe for both the serpentine-type antenna and the double comb-type antenna as a function of antenna position at 2000 W of rf power with an Ar pressure of 15 mTorr. The measured positions along both antennas are also shown. As shown, in the serpentine-type antenna, the rf rms voltage measured from the rf power input position to the ground position increased along the antenna line and showed a peak at a certain position. However, in the case of the double comb-type antenna, the voltages measured at the same locations were similar and no peak in the rf rms voltage was observed. Also, the rf rms voltages measured for the double comb-type antenna were generally lower than those for the serpentine-type antenna. The observed voltage peak in the serpentine-type antenna appeared from the standing wave effect due to the longer length of the antenna. In fact, the antenna voltage along the antenna position shown in the figure for the double comb-type antenna is not the voltage distribution along the antenna line while that for the serpentine-type antenna can be regarded as the rf voltage distribution along the antenna line; therefore, the data

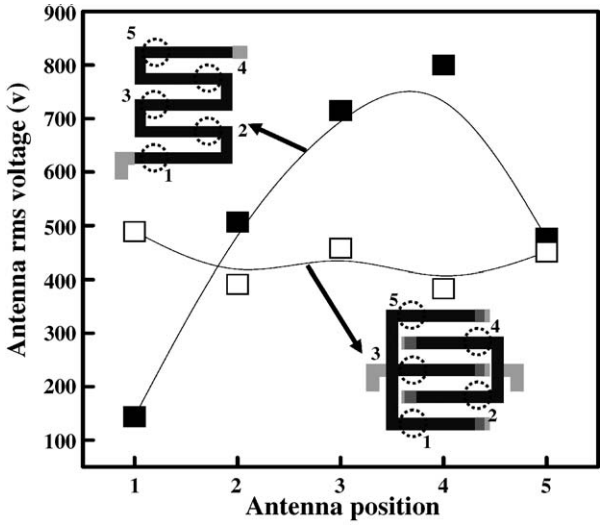

Fig. 2. Rf rms voltage distribution of the serpentine-type and the double comb-type antennas along the antenna line measured by a high voltage probe at 2000 W of rf power with 15 mTorr of Ar.

cannot be directly compared. However, the data shown in Fig. 2 is believed to show the more standing wave effect and higher antenna voltage for the serpentine-type antenna compared to the double comb-type antenna.

Fig. 3 shows the rf rms antenna voltage near the rf power input location (that is, the location at the matching network which is 30 cm distance from the location 1 in the Fig. 2) as a function of rf power from 1000 to 5000 W measured by a V–I probe. An Ar pressure of 15 mTorr was also used for the experiment. As shown in the figure, the measured antenna voltage was increased with increasing rf power for both the serpentine–type and the double comb-type antennas. However, over the whole range of investigated rf power, the antenna voltage of the serpentine-type antenna

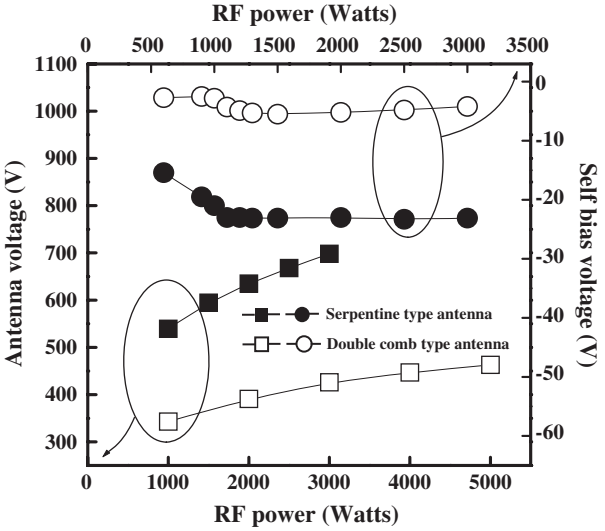

Fig. 3. Rf rms voltages of the antenna (at the matching network position) and dc bias voltages on the quartz tubing enclosing the antenna for the serpentine-type and double comb-type antenna measured using a high voltage probe as a function of rf power from 250 W to 5000 W at 15 mTorr of Ar.

was higher at the same rf power and increased faster with rf power compared to that of the double comb-type antenna due to the higher impedance of the serpentine-type antenna. Fig. 3 also shows the dc voltage measured on the surface of the quartz tubing as the rf power ranged from 250 to 3000 W with 15 mTorr Ar. The measured dc voltage for the serpentine-type antenna was increased with increasing rf power to peak at about 24 V with an rf power of 3000 W. However, in the case of the double comb-type antenna, the dc voltage remaining similar near 0 V, without any significant change, as rf power increased and the highest dc voltage was less than 5 V in general. The dc voltage measured on the quartz tubing is related to the voltage developed between the quartz tubing and the plasma by the capacitive coupling. Therefore, the higher dc voltages measured for the serpentine-type antenna suggest the higher capacitive coupling to the plasma due to the higher rf voltage on the antenna. In addition, the quartz tubing can be bombarded by the ions accelerated by this dc voltage, and this high dc voltage on the quartz tubing will therefore cause erosion of the quartz tubing by the sputter etching and possible contamination to the chamber. In the case of dc voltage induced on the quartz plate, it is related to the rf antenna voltage (V_a) from the following equation [13],

$$V_{DC} \alpha V_s \cong \frac{C_i}{C_i + C_s} V_a$$

where, C_i is the capacitance between the antenna and quartz surface, C_s is the capacitance between the quartz surface and the plasma. The lower dc voltage on the surface of quartz tubing is related to the lower antenna voltage and, in our experiment, it is also related to the higher antenna current at a given rf power which is required for the inductive coupling. Therefore, it is believed that the lower dc voltage on the surface of quartz tubing at a given rf power should be related to the more effective inductive coupling to the plasma.

Because the double comb-type antenna showed better characteristics than the serpentine-type antenna, the densities of the plasmas and the etch rates of photoresist and SiO_2 were measured for the double comb-type antenna as a function of rf power ranging from 1000 to 5000 W using 15 mTorr of Ar and SF_6, respectively. The results are shown in Fig. 4. The plasma density was measured 7.5 cm below the plasma source at the center of the chamber using a Langmuir probe and the etch rates of photoresist and SiO_2 were measured at the center of the substrate. The substrate holder was located about 5 cm below the plasma source. During the etching, the substrate dc-bias voltage was fixed at −60 V. As shown in the figure, the plasma density increased almost linearly with increasing rf power to peak at about $2.3 \times 10^{11}/cm^3$ at 5000 W of rf power. When the etch rates of photoresist and SiO_2 were measured using 15 mTorr of SF_6 and −60 V of dc-bias voltage, they also increased almost linearly with increasing rf power, to peak at 3000 Å/min and 1500 Å/min, respectively, at 5000 W of rf power.

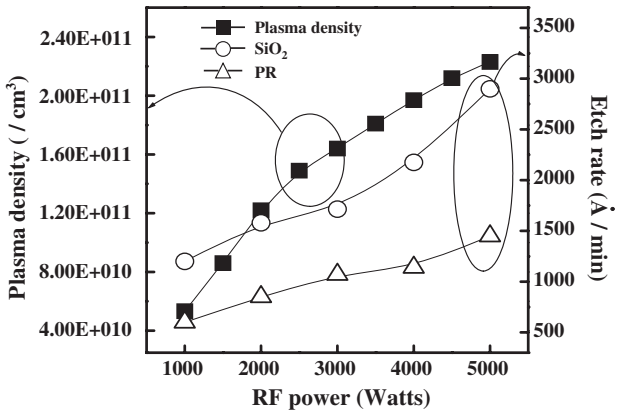

Fig. 4. Ar plasma density and etch characteristics of photoresist and SiO_2 as a function of rf power ranging from 1000 to 5000 W at 15 mTorr of Ar and SF_6, respectively. For the etching, dc-bias voltage was maintained at −60 V.

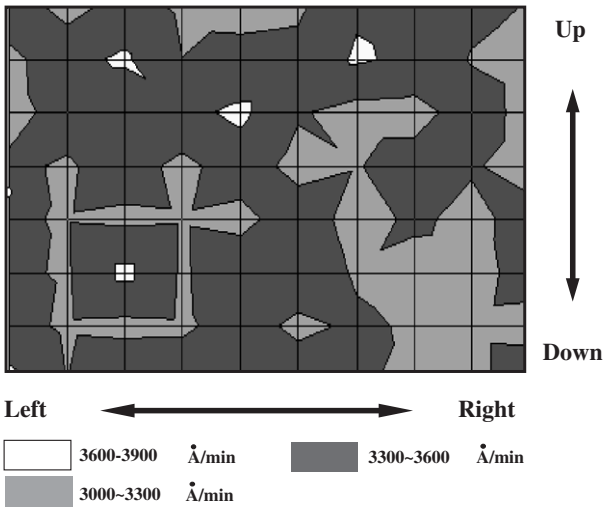

Fig. 5. Etch uniformity of photoresist measured at 5000 W of rf power, −60 V of dc-bias voltage, and 15 mTorr of O_2 for the substrate sized 880 mm × 660 mm.

The etching was carried out at 5000 W of rf power, −60 V of dc-bias voltage, and 15 mTorr O_2, and the result is shown in Fig. 5. As shown in the figure, the etch rates on the 880 mm × 660 mm substrate were not significantly different and, at this condition, an etch uniformity of about 7% could be obtained.

4. Conclusions

In this study, the serpentine-type antenna showed higher rf rms voltages on the antenna and a higher dc voltage on the surface of the quartz tubing, compared to the double comb-type antenna, over the complete range of rf power due to the higher impedance of the antenna. Furthermore, when the antenna voltage was measured along the antenna line, the serpentine-type antenna showed a peak voltage at a certain position between the power input and the ground possibly indicating the standing wave effect due to the long

length of the antenna. In contrast, the double comb-type showed similar rf rms voltages at the same locations.

Acknowledgments

This work was supported by the NRL Program of the Korea Ministry of Science and Technology.

References

[1] F. Mendoza, B. Sarette, D. McReynolds, B. Richardson, J. Holland, Semicond. Int. (1999 June) 143.
[2] C.Y. Chang, S.M. Sze, ULSI Technology, McGraw-Hill, New York, 1996, p. 329.
[3] J.L. Crowley, Solid State Technol. 35 (1992) 94.
[4] M.A. Lieberman, A.J. Lichtenberg, Principles of Plasma Discharges and Materials Processing, John Wiley & Sons Inc., New York, 1994.
[5] P.L.G. Ventzek, T.J. Sommerer, R.J. Hoekstra, M.J. Kushner, Appl. Phys. Lett. 63 (1993) 605.
[6] J.H. Keller, Plasma Phys. Control. Fusion A 39 (1997) 437.
[7] M.H. Khater, L.J. Overzet, J. Vac. Sci. Technol., A, Vac. Surf. Films 19 (2001) 785.
[8] J. Yu, D. Shaw, P. Gonzales, G.J. Collins, J. Vac. Sci. Technol., A, Vac. Surf. Films 13 (1995) 871.
[9] Hikaru Kokura, Keiji Nakamura, Ivan P. Ghanashev, Hideo Sugai, Jpn. J. Appl. Phys. 38 (1999) 5262.
[10] Y. Wu, M.A. Lieberman, Plasma Sources Sci. Technol. 9 (2000) 210.
[11] M. Kahoh, K. Suzuki, J. Tonotani, K. Aoki, M. Yamage, Jpn. J. Appl. Phys. 40 (2001) 5419.
[12] Y. Setsuhara, T. Shoji, A. Ebe, S. Baba, N. Yamamoto, K. Takahashi, K. Ono, S. Miyake, Surf. Coat. Technol. 174–175 (2003) 33.
[13] Y. Wu, M.A. Lieberman, Plasma Sources Sci. Technol. 9 (2000) 210.